Integrated FCC Riser - Regenerator Dynamics studied in a Fluid Catalytic Cracking Pilot Plant

G. M. Bollas[*] *and I. A. Vasalos*

Laboratory of Petrochemical Technology, Department of Chemical Engineering, Aristotle University of Thessaloniki, PO Box 361, 57001, Thessaloniki, Greece

A. A. Lappas, D. K. Iatridis, S. S Voutetakis

Chemical Process Engineering Research Institute (CPERI), Centre for Research and Technology Hellas (CERTH), PO Box 361, 57001, Thermi-Thessaloniki, Greece

S. A. Papadopoulou

Automation Department, Alexander Technological Educational Institute of Thessaloniki, P.O. Box 14561, GR54101, Thessaloniki, Greece

[*] Corresponding author. Chemical Process Engineering Research Institute, Centre for Research and Technology Hellas, 6th km. Charilaou – Thermi Rd., PO Box 361, Thessaloniki, GR-570 01, Greece, Fax: +30 2310 498380, E-mail: gbollas@cperi.certh.gr

Abstract

In this paper a dynamic simulator of the FCC pilot plant, operated in Chemical Process Engineering Research Institute (CPERI), is presented. The simulator was developed and verified on the basis of steady-state and dynamic experiments. The operation of the pilot plant permits the execution of case studies for recording of the dynamic responses of the unit, by imposing substantial step changes in a number of the manipulated variables. The comparison between the dynamic behavior of the unit and this predicted by the simulator, arise useful conclusions on both the similarities of the pilot plant to commercial units along with the ability of the simulator to depict the main dynamic characteristics of the integrated system. The simulator predicts the wt% feed conversion, the wt% coke yield and the heat consumed by the catalytic reactions in the FCC riser on the basis of semi-empirical models developed in CPERI and simulates the regenerator according to the two-phase theory, with a dilute phase model in account for post-combustion reactions. The riser and regenerator temperature, the stripper and regenerator pressure drop and the composition of the regenerator flue gas are measured on line and are used for verification of the ability of the simulator to predict the dynamic transients between steady states in both open- and closed-loop unit operation. All the available process variables such as the reaction conversion, the coke yield, the carbon on regenerated catalyst and the catalyst circulation rate are used for the validation of the steady state performance of the simulator. The results reveal the ability of the simulator to predict accurately the operation of the pilot plant in both steady state and dynamic conditions. The dynamic simulator can serve as the basis for the development of a model based control structure for the pilot plant, besides its use as a tool for process optimization studies.

Keywords: Fluid Catalytic Cracking, Mathematical Modeling, Dynamic Simulation, Pilot Plant, Catalyst Deactivation, Bubble Columns

Introduction

The dynamic simulation of the Fluid Catalytic Cracking (FCC) process is a challenging research subject of high economic and environmental importance. Optimization of this complex process demands the development of accurate models capable of describing the process in detail. FCC technology is continuously evolving during the last half century, though the requirements for stable operation of commercial FCC units restrict the possibility of obtaining accurate models over an extensive operating range, through experimentation. In industry the target is maximum capacity (i.e. profitability), and that bounds the evidence of dynamic transients within particular and narrow operating windows. Thus, FCC pilot plants are often used for the simulation of commercial units under different operating conditions, feed properties and catalyst activity and selectivity. The operation of a pilot unit provides the ability to examine the process under steady feed and/or catalyst properties, in order to isolate their respective effects on the cracking reactions and develop correlations for each subset of process variables. One other asset of FCC pilot plants is the potential to examine their dynamic behavior within a great range of operating conditions, which enhances the investigation of the process dynamics.

The research interest in dynamic simulation of the fluid catalytic cracking process has been consecutively increasing during the last years. Lee and Groves (Lee & Groves, 1985) proposed a dynamic model which treats the riser as a pseudo-steady state adiabatic plug flow reactor and the regenerator as a continuous stirred tank reactor with no dilute phase. Elnashaie et al. (Elnashaie, Abasaeed & Elshishini, 1995; Elnashaie & Elshishini, 1993) developed a dynamic model for an industrial type IV FCC unit and investigated the sensitivity and stability of the system. They used two-phase models for both the reactor and the regenerator and included unsteady state dynamic terms for the thermal behavior and for the carbon mass balance throughout the entire unit. Lopez-Isunza (Lopez-Isunza, 1992) presented a dynamic model for mass and energy balance, but their model neglects the hydrodynamic aspects of the

FCC unit. McFarlane et al. (McFarlane et al., 1993) presented a comprehensive model for the simulation of a type IV FCC unit, in which they included the reactor, regenerator, blowers, U-bends, compressors, furnace and valves, as to be able to compute the pressure balance and catalyst circulation rate of this type of unit. In the regenerator model they included a dilute phase in account for post combustion, but the riser part used oversimplified computations for the heat balance. Arbel et al. (Arbel et al., 1995; Arbel, Rinard & Shinnar, 1995) developed a model able to describe both the steady-state and dynamic behavior of an FCC unit. Their riser model was based on the widely known 10-lump model (Jacob et al., 1976), assuming pseudo-steady state conditions, while the regenerator model included a complete description of both full and partial combustion kinetics. They extensively studied the steady state multiplicities of the FCC unit and the effect of combustion mode on the controllability of the unit. Ali and Rohani (Ali & Rohani, 1997; Ali, Rohani & Corriou, 1997) presented a dynamic model, in which they developed analytical solutions of the differential model equations after adopting pseudo-steady state assumptions. Their model neglects the freeboard region of the regenerator. In-Su Han et al. (Han & Chung, 2001a, , 2001b) presented a detailed dynamic simulator of the FCC process, in which they included the simulation of catalyst liftlines, stripper, feed preheater and cyclones. They applied a distributed parameter 4-lump model for the riser reactor and a two-regime, two-phase model for the regenerator. The UOP type fluid catalytic cracking unit was in detail simulated by Cristea et al. (Cristea, Agachi & Marinoiu, 2003). The simulator of Cristea et al. is based on the model of McFarlane et al. (McFarlane et al., 1993) including models for the feed preheater, the main fractionator, the air blower, the wet gas compressor. Cristea et al. implemented model predictive control (MPC) algorithm to their simulator and studied the effect of the control structure on the unit performance. Recently, Hernandes-Barajas et al. (Hernandez-Barajas, Vazquez-Roman & Salazar-Sotelo, 2006) presented another dynamic simulator of the FCC unit, with a detailed pressure balance

of the unit. Hernandes-Barajas et al. focused on the multiplicity of steady states in fluid catalytic cracking units.

In this paper the development and verification of a dynamic simulator, on the basis of steady-state and dynamic experimental data of the FCC pilot plant of Chemical Process Engineering Research Institute (CPERI), will be presented. The term “dynamic experiments” is used to describe experiments, in which a step change is imposed to a manipulated process variable, while recording the transient of a number of process variables from the original steady state to the final steady state the system will eventually reach. The development of the dynamic simulator of the pilot plant serves two main goals: a) the study of the dynamic behavior of the pilot process that includes the validation of the model performance against steady-state and dynamic unit responses, the identification of the process dependencies and uncertainties, and the performance of experimental case studies to examine the similarities of the pilot plant with commercial units, and b) the use of the simulator for the development of a model-based optimizer and control scheme for the entire unit. This paper deals with the former of the aforementioned goals and examines the ability of the simulator to provide an accurate representation of the unit qualitatively and quantitatively, as well as the ability of both the pilot plant and the simulator to simulate the main dynamic characteristics of a typical commercial FCC process.

Experimental Setup

The FCC pilot plant of CPERI (Fig. 1) operates in a fully circulating mode and consists of a riser reactor, a fluid bed regenerator, a stripper and a liftline. The riser reactor operates at pseudo-isothermal plug flow conditions and consists of a large-diameter bottom region (mixing zone) (26mm i.d., 0.3m height) and a smaller-diameter (7mm i.d., 1.465m height) top region connected by a conical-shaped region 0.05m of height. At the reactor bottom, the gas-oil contacts the hot catalyst (which flows from the regenerator) and evaporates, while the catalyst is kept in a fluidized state by means of nitrogen flow. The cracking product from the riser top enters the stripper vessel for the separation (stripping) of gas from catalyst. The stripped mixture flows through a heat exchanger for condensation of the heavier compounds. Thereupon, the mixture is led to a stabilizer column for better separation of the liquid and gaseous products. The mixture of gasoline, light cycle oil and heavy cycle oil is obtained through the bottom of the stabilizer. The yield to liquid products is measured with the ASTM D-2887 simulated distillation method. The stripped catalyst flows through the liftline to the regenerator, where the majority of the carbon, deposited on the catalyst surface, is burned off. The regenerator consists of two main sections. A small-diameter bottom section (77.92mm i.d., 0.715m height) and a larger-diameter top section (254.6mm i.d., 0.64m height) connected by a conical-shaped section 0.205m of height. A standpipe at the bottom of the regenerator leads the regenerated catalyst back to the riser bottom to continue the operation loop. Two slide valves, one at the exit of the standpipe and one at the exit of the stripper regulate the catalyst circulation throughout the unit. The standpipe slide valve controls the catalyst circulation for constant riser temperature, while the stripper slide valve operates for constant stripper pressure drop (i.e. stripping volume). Two wet test meters and two gas chromatographers measure the volumetric flow rates and the molar composition of the flue and cracked gas, respectively. An on-line oxygen analyzer monitors the excess of oxygen to ensure thorough catalyst regeneration. The process control system of the unit is based on a

special industrial computer control system. The system is coordinated with the FIX/DMACS S/W by Intellution. The control system collects the values of the inputs and drives the output signals, as well as maintains a digital record of the signals. The process pressure control valves and the power to electrical heaters are controlled by numerous PID controllers.

Model Description

The simulator of the pilot plant includes three main sections: a pseudo-steady state model of the riser reactor, a dynamic model of the regenerator and a set of dynamic and pseudo-steady state models of the stripper, the standpipe, the liftline and the slide valves. For the specific case of the pilot plant, the dynamic effects of the riser, the cyclones, the liftline and the standpipe on the performance of the integrated unit were neglected, because their operation has significantly lower impact on the process dynamics, compared to the two large vessels of the pilot plant, the stripper and the regenerator. The behavior of the regenerator dominates on both the dynamic and the steady state behavior of the integrated unit. This is due to the adiabatic nature of the system in which the need to balance coke formation and combustion is the predominant force (Arbel et al., 1995). The riser residence times are much shorter compared to the response times of the regenerator, hence one can at any instance describe the riser reactor by a set of pseudo-steady state equations, which simplifies the dynamic analysis. The main impact of the riser operation on both the dynamic and steady state behavior of the integrated system is on the coke production and on the heat consumption. Thus, the accurate prediction of pseudo-steady state conversion, coke yield and heat of cracking and vaporization is the main concern, when describing the effect of riser in the integrated dynamic system.

The pseudo-steady state and dynamic sub-models that constitute the dynamic simulator, as developed in CPERI, have been presented in the literature (Bollas et al., 2002; Bollas et al., 2004; Faltsi-Saravelou & Vasalos, 1991; Faltsi-Saravelou, Vasalos & Dimogiorgas, 1991) and will be briefly adduced in this section. A kinetic-hydrodynamic model was developed for the simulation of the pilot riser reactor in pseudo-steady state conditions (Bollas et al., 2002). The catalyst hold-up and residence time in the reactor were calculated on the basis of empirical hydrodynamic correlations and the gas-oil conversion and coke yield were predicted through a Blanding type (Blanding, 1953) kinetic model. The prediction of gas-oil

conversion and coke yield are the only two lumps of the riser sub-model, essential for inclusion in the complete simulator, which reduces the necessity of using a more detailed lumped model. The effect of feedstock properties on gas-oil conversion and coke yield was expressed through semi-empirical correlations developed on the basis of experiments performed with constant catalyst and a variety of feedstocks (Bollas et al., 2004). The effect of catalyst type was expressed through a "catalyst index" (Bollas et al., 2004). The model of the regenerator is based on the two-phase theory (Davidson, Clift & Harrison, 1985), in which the gas-solids flow is assumed to follow the bubbling bed regime, consisting of two zones: a dense zone at the regenerator bottom comprised by a bubble and an emulsion phase, and a dilute zone at the regenerator top, called the freeboard. The model equations were grouped into two main modules that serve for the two main sections of the unit, the riser and the regenerator. A third module was used for the simulation of the stripper and the slide valves, the liftline and the standpipe.

Simulation of Riser Reactor

The pseudo-steady state model of the FCC riser reactor was developed on the basis of the following assumptions:

- the aggregate effect of operating conditions, feed properties and catalyst type on the cracking reactions are simulated by the product of their discrete functions
- the riser reactor is assumed to run in concurrent plug flow of gas and solids at pseudo-isothermal conditions
- second-order rate apparent kinetics are applied for gas-oil conversion (x)
- catalytic coke (c_x) deposition parallels catalyst deactivation (Voorhies, 1945).

On the basis of these assumptions and after integration and rearrangement of the corresponding spatial equations eqs.(1) and (2) were formulated:

$$\frac{x}{100-x} = C\left(catalyst\ type\right) F\left(feed\ quality\right) \frac{k_x}{WHSV} \exp\left(\frac{-E_x}{R_g T_{RX}}\right) t_{C:\mathrm{RS}}{}^{n_x} \tag{1}$$

$$c_x = C_c\left(catalyst\ type\right) F_c\left(feed\ quality\right) \frac{k_c}{WHSV} \exp\left(\frac{-E_c}{R_g T_{RX}}\right) t_{C:\mathrm{RS}}{}^{n_c} \tag{2}$$

The adjustable parameters (k_x, k_c, E_x, E_c, n_x, n_c) of eqs.(1) and (2) were estimated on the basis of a dataset of steady state pilot experiments performed with constant feed and catalyst quality, in a great range of space velocities (*WHSV*) and catalyst residence times ($t_{C:\mathrm{RS}}$) and at two different reactor temperatures (T_{RX}) (Bollas et al., 2002). A large database of experiments with different feedstocks and catalysts was used for the development of models of the effect of feedstock quality and the assignment of "catalyst indices" that are used in eqs.(1) and (2). The methodology of the simulation of the effect of feed and catalyst on conversion and coke yield is shortly described in Appendix B. The values of the parameters of eqs.(1) and (2) are given in Table 1.

Finally, a pseudo-steady state heat balance of the riser reactor was performed. The main contributors to the overall enthalpy balance in an FCC plant are: (a) the enthalpy of cracking ΔH_{crack}; (b) the enthalpy of vaporization of the gas-oil feedstock; and (c) the enthalpy content of various process streams (gas-oil, catalyst, cracked products, inerts). An empirical correlation was developed to estimate the heat of cracking in the riser reactor. This correlation was based on experiments performed at different temperatures, using various feedstocks and at different conversion levels. The final correlation estimates the heat of cracking as a function of conversion, riser temperature and gas-oil molecular weight, as shown in eq.(3):

$$\Delta H_{crack} = \ln\left(\frac{x}{100-x}\right)\left(a_1 T_{RX} + a_2 T_{RX}{}^2 + a_3 MW_F\right) + \left(b_1 T_{RX} + b_2 T_{RX}{}^2 + b_3 MW_F\right) \tag{3}$$

The enthalpy content of gas-oil vapors was estimated by integration of the empirical correlation of Kesler and Lee (Kesler & Lee, 1976). The values of the parameters of eq.(3) are presented in Table 1.

Simulation of Regenerator

The structure of the physical model of the regenerator is shown in Fig. 2. The fluidized bed includes two zones: (a) the dense bed and (b) the freeboard. The dense bed consists of a bubble and an emulsion phase, while the freeboard contains the entrained catalyst particles that are recycled to the emulsion phase of the dense zone via cyclones.

The assumptions made for the simulation of each phase shown in Fig. 2 are (Faltsi-Saravelou & Vasalos, 1991; Faltsi-Saravelou, Vasalos & Dimogiorgas, 1991):

- the bubble phase is free of catalyst particles
- plug flow regime is assumed for the bubble phase
- the emulsion phase gas and catalyst particles are assumed fully mixed
- the freeboard is modeled as an ideal plug flow reactor
- the catalyst particles are hydrodynamically represented by their average size, density and porosity, while the particle size distribution is used for the emulsion to freeboard entrainment rate calculation
- diffusion in the catalyst particles is neglected
- due to the high temperatures in the FCC regenerator, the ideal gas law is valid
- the fluidized bed reactor is adiabatic.

The velocity of the gas flowing through the emulsion phase, was assumed to be equal to the minimum bubbling velocity, which is a consistent assumption for Geldart group A particles (Geldart, 1973) (in which category FCC catalysts typically belong). The clouds and wakes around the bubbles were assumed to have zero volume. This assumption is valid for high ratios of superficial gas velocity over minimum fluidization velocity, which is typical for operations of group A particles. The bubbles were assumed to grow in size with bed height, while the variation of the fluidizing gas density and superficial velocity, due to axial temperature gradients and gas molar rate changes, was also taken into account.

The dense bed of the regenerator was simulated as a pseudo-steady state PFR (bubble phase) in parallel to a dynamic CSTR (emulsion phase). The dense bed volume was calculated on the basis of the overall regenerator dynamics:

$$\frac{dV_{D:\mathrm{RG}}}{dt} = \frac{\dot{W}_{C:\mathrm{RG}}^{(l_D=1)} - \dot{W}_{C:\mathrm{RG}}^{(l_D=0)} + \dot{W}_{C:\mathrm{CY}}^{(l_F=1)} - \dot{W}_{C:\mathrm{CY}}^{(l_F=0)}}{\rho_p \left(1-\varepsilon_e\right) f_e} \tag{4}$$

The material balance for gas components in the bubble phase is:

$$\frac{1}{V_{D:\mathrm{RG}}} \frac{dF_{ib}}{dl_D} = -K_{Mi} + f_b \sum_j^{homo} a_{ij} K_{Rjb} \tag{5}$$

The energy balance in the bubble phase is given by eq.(6):

$$\frac{1}{V_{D:\mathrm{RG}}} \frac{dQ_b}{dl_D} = -K_H + f_b \sum_j^{homo} \left(-\Delta H_{Rj}\right) K_{Rjb} \tag{6}$$

In the emulsion phase the material balance equations were formulated separately for gas and solids components, as shown in eqs.(7) and (8) respectively:

$$f_e \varepsilon_e \frac{dc_{ie}}{dt} = \frac{\dot{W}_{ge}^{(l_D=0)}}{\rho_{ge}} \frac{c_{ie}^{(l_D=0)} - c_{ie}}{V_{D:\mathrm{RG}}} + \int_0^1 K_{Mi} dl_D + f_e \varepsilon_e \sum_j^{homo} a_{ij} K_{Rje} + f_e \left(1-\varepsilon_e\right) \sum_j^{hete} a_{ij} K_{Rje} \tag{7}$$

$$f_e \left(1-\varepsilon_e\right) \frac{dc_{ie}}{dt} = \frac{\dot{W}_{C:\mathrm{RG}}^{(l_D=1)}}{\rho_p} \frac{c_{ie}^{(l_D=1)} - c_{ie}}{V_{D:\mathrm{RG}}} + \frac{\dot{W}_{C:\mathrm{CY}}^{(l_F=1)}}{\rho_p} \frac{c_{if}^{(l_F=1)} - c_{ie}}{V_{D:\mathrm{RG}}} + f_e \left(1-\varepsilon_e\right) \sum_j^{hete} a_{ij} K_{Rje} \tag{8}$$

The energy balance equation in the emulsion phase is given by eq.(9):

$$\begin{aligned} &\left(f_e \left(1-\varepsilon_e\right) \sum_i^{solids} c_{ie} cp_{ie} + f_e \varepsilon \sum_i^{gas} c_{ie} cp_{ie} \right) \frac{d\left(V_{D:\mathrm{RG}} T_e\right)}{dt} = Q_{C:\mathrm{RG}}^{(l_D=1)} - Q_{C:\mathrm{RG}}^{(l_D=0)} + Q_{C:\mathrm{CY}}^{(l_F=1)} - Q_{C:\mathrm{CY}}^{(l_F=0)} + Q_{ge}^{(l_D=0)} \\ &- Q_{ge}^{(l_D=1)} - Q_{loss} + V_{D:\mathrm{RG}} \int_0^1 K_H dl_D + f_e \varepsilon_e V_{D:\mathrm{RG}} \sum_j^{homo} \left(-\Delta H_{Rj}\right) K_{Rje} + f_e \left(1-\varepsilon_e\right) V_{D:\mathrm{RG}} \sum_j^{hete} \left(-\Delta H_{Rj}\right) K_{Rje} \end{aligned} \tag{9}$$

The superficial bubble gas velocity for the dimensionless fraction of dense bed height l_D, is evaluated by differentiating the ideal gas law in terms of the bubble enthalpy rate term:

$$\frac{du_{gb}}{dl_D} = \frac{R_g}{A_{D:\mathrm{RG}} P_{D:\mathrm{RG}} \overline{cp}_{gb}} \frac{dQ_b}{dl_D} \tag{10}$$

The bubble-emulsion mass interchange K_{Mi} and the heat interchange K_H and the emulsion fraction f_e are evaluated by eqs. (11) - (13), respectively:

$$K_{Mi} = K_{ti}\left(\frac{F_{ib}}{u_{gb}A_{D:\mathrm{RG}}} - c_{ie}\right) \tag{11}$$

$$K_H = H_t\left(T_b - T_e\right) \tag{12}$$

$$f_e = \int_0^1 \left(1 - f_b\right) dl_D \tag{13}$$

The combined bubble to emulsion gas interchange coefficients are evaluated by eq.(14):

$$\frac{f_b}{K_{ti}} = \frac{1}{k_{bci}} + \frac{1}{k_{cei}} \tag{14}$$

For the evaluation of the bubble-cloud (k_{bci}) and cloud-emulsion (k_{cei}) gas interchange coefficients the expressions proposed by Kunii and Levenspiel (Kunii & Levenspiel, 1977) were adopted. The same method (Kunii & Levenspiel, 1977) was used for the estimation of the heat interchange coefficient (H_t).

The freeboard is simulated as an ideal two-phase PFR. The material balances of the gas and solid components in the freeboard are shown in eqs. (15) and (16), respectively:

$$\frac{1}{V_{F:\mathrm{RG}}}\frac{dF_{if}}{dl_F} = \varepsilon_f \sum_j^{homo} \alpha_{ij} K_{Rjf} + \left(1 - \varepsilon_f\right)\sum_j^{hete} \alpha_{ij} K_{Rjf} \tag{15}$$

$$\frac{1}{V_{F:\mathrm{RG}}}\frac{dF_{if}}{dl_F} = \left(1 - \varepsilon_f\right)\sum_j^{hete} \alpha_{ij} K_{Rjf} \tag{16}$$

The energy balance for the freeboard is:

$$\frac{1}{V_{F:\mathrm{RG}}}\frac{dQ_f}{dl_F} = \varepsilon_f \sum_j^{homo} \left(-\Delta H_{Rj}\right) K_{Rjf} + \left(1 - \varepsilon_f\right)\sum_j^{hete} \left(-\Delta H_{Rj}\right) K_{Rjf} \tag{17}$$

The ideal gas law is differentiated in terms of the gas enthalpy rate to evaluate the gas superficial velocity:

$$\frac{du_{gf}}{dl_F} = \frac{R_g}{A_{F:\mathrm{RG}} P_{F:\mathrm{RG}} \overline{cp}_{gf}} \frac{dQ_{gf}}{dl_F} \tag{18}$$

The derivative of the enthalpy of the gas phase is obtained by eq.(19), assuming that the heat capacity of the components is constant at each integration step:

$$\frac{dQ_{gf}}{dl_F} = \frac{Q_{gf}}{Q_f}\frac{dQ_f}{dl_F} \tag{19}$$

The chemical species considered to be involved in the reaction scheme of the regenerator are categorized to gas components (N_2, O_2, CO_2, CO, H_2O) and solid components (Al_2O_3, SiO_2, C, H, S). A short description of the kinetics of the heterogeneous and homogeneous reactions is given in (R1)–(R6):

The intrinsic carbon combustion on the catalyst surface corresponds to a couple of reactions producing CO and CO_2 with second order kinetics:

$$\mathrm{C} + \frac{1}{2}\mathrm{O_2} \xrightarrow{K_1} \mathrm{CO} \qquad r_1 = K_1[\mathrm{C}][\mathrm{O_2}] \qquad \text{(R1)}$$

$$\mathrm{C} + \mathrm{O_2} \xrightarrow{K_2} \mathrm{CO_2} \qquad r_2 = K_2[\mathrm{C}][\mathrm{O_2}] \qquad \text{(R2)}$$

The homogeneous CO oxidation in the gas phase, at which the water acts catalytically:

$$\mathrm{CO} + \frac{1}{2}\mathrm{O_2} \xrightarrow{K_3} \mathrm{CO_2} \qquad r_3 = K_3[\mathrm{O_2}]^{0.5}[\mathrm{CO}][\mathrm{H_2O}]^{0.5} \qquad \text{(R3)}$$

The catalytic CO oxidation, at which part of the CO produced on the catalyst site, is catalytically oxidized on the catalyst itself, or on an oxidation promoter:

$$\mathrm{CO} + \frac{1}{2}\mathrm{O_2} \xrightarrow{K_4} \mathrm{CO_2} \qquad r_4 = K_4[\mathrm{CO}] \qquad \text{(R4)}$$

The hydrogen combustion on the catalyst surface, which produces a significant amount of heat, is:

$$2\mathrm{H} + \frac{1}{2}\mathrm{O_2} \xrightarrow{K_5} \mathrm{H_2O} \qquad r_5 = K_5[\mathrm{H}][\mathrm{O_2}] \qquad \text{(R5)}$$

The coke sulfur combustion on the catalyst, which produces mainly SO_2, is:

$$\mathrm{S} + \mathrm{O_2} \xrightarrow{K_6} \mathrm{SO_2} \qquad r_6 = K_6[\mathrm{S}][\mathrm{O_2}] \qquad \text{(R6)}$$

The reaction of C and CO_2 on the catalyst site producing CO is neglected, as it occurs at a very low rate. The parameters of the kinetic expressions (R1)-(R6) are presented in Table 2.

Simulation of Stripper, Standpipe, Liftline and Slide Valves

The stripper was simulated as a perfectly mixed reactor in minimum fluidization conditions, the reactor dense bed volume of which and the material balance for the solids components were expressed through eqs.(20) and (21):

$$\frac{dV_{D:\mathrm{ST}}}{dt} = \frac{\dot{W}_{C:\mathrm{ST}}^{(l_D=1)} - \dot{W}_{C:\mathrm{ST}}^{(l_D=0)}}{\rho_p \left(1-\varepsilon_{mf}\right)} \tag{20}$$

$$\frac{dc_{i:\mathrm{ST}}}{dt} = \frac{\dot{W}_{C:\mathrm{ST}}^{(l_D=1)} \left(c_{i:\mathrm{ST}}^{(l_D=1)} - c_{i:\mathrm{ST}}\right)}{\rho_p \left(1-\varepsilon_{mf}\right) V_{D:\mathrm{ST}}} \tag{21}$$

The stripping efficiency of the pilot stripper was assumed 100%, as the stripper volume and the stripping steam flow are adequately large for the pilot riser capacity. In the pilot plant the temperature of the catalyst at the stripper dense bed is regulated by electrical heaters, that operate to achieve a set point value. The temperature of the catalyst stream at the exit of the standpipe (riser entrance) and at the exit of the liftline (regenerator entrance) is calculated by eq.(22):

$$\frac{dT}{dl} = \frac{\left(T_w - T\right)}{cp_C} \frac{\pi DL}{\dot{W}_C} \tag{22}$$

Model Structure – Initial and Boundary Conditions

The dynamic material and energy balance equations form a system of integro-differential equations that is solved following an iterative procedure commencing from the initial and boundary conditions of the system, as shown in Fig. 3. The common case is that the simulator is used to study the transient from a simulated steady state of the unit to a new one, when a step change is imposed to one ore more of the manipulated variables. Otherwise, the system variables receive the starting values of a "guess" steady state, estimated on the basis of the assumption of plug flow conditions throughout the regenerator. Thereafter, the system is solved until convergence to a valid steady state. For time zero the emulsion variables

($c_{ie}^{(t=0)}$, $V_{D:\mathrm{RG}}^{(t=0)}$, $T_e^{(t=0)}$ and all other time dependent variables shown in Fig. 3) hold the values of the initial steady state. The superficial gas velocity at the regenerator entrance, $u_{g:\mathrm{RG}}^{(l_D=0)}$, is calculated using the ideal gas low for combustion air flow rate $\dot{W}_{g:\mathrm{RG}}^{(l_D=0)}$ at temperature $T_b^{(l_D=0)}$ equal to the air preheat temperature and pressure $P_{D:\mathrm{RG}}^{(l_D=0)}$ equal to the regenerator bottom pressure. The superficial gas velocity in the bubbles at the entrance of the regenerator is then calculated by eq.(23), where $u_{ge}^{(t)}$ is the superficial gas velocity in emulsion at real time t ($t = 0$ for the initial steady state):

$$u_{gb}^{(l_D=0)} = u_{g:\mathrm{RG}}^{(l_D=0)} - u_{ge}^{(t)} \tag{23}$$

For the dilute phase, the boundary conditions at the dimensionless height $l_F = 0$ (end of the dense zone entrance to the freeboard region) are:

$$F_{if}^{(l_F=0)} = F_{ib}^{(l_D=1)} + c_{ie}^{(t)} u_{ge} A_{D:\mathrm{RG}} \tag{24}$$

$$F_{if}^{(l_F=0)} = c_{ie}^{(t)} u_{sf}^{(l_F=0)} A_{F:\mathrm{RG}} \tag{25}$$

$$Q_f^{(l_F=0)} = Q_b^{(l_D=1)} + \left(\sum_i^{solids} c_{ie}^{(t)} u_{sf}^{(l_F=0)} A_{F:\mathrm{RG}} cp_{ie} + \sum_i^{gas} c_{ie}^{(t)} u_{ge}^{(l_D=1)} A_{D:\mathrm{RG}} cp_{ie} \right) \left(T_e - T_r \right) \tag{26}$$

$$u_{gf}^{(l_F=0)} = \left(u_{gb}^{(l_D=1)} + u_{ge}^{(t)} \right) \frac{A_{D:\mathrm{RG}}}{A_{F:\mathrm{RG}}} \tag{27}$$

The catalyst with concentration $c_{ie}^{(t)}$ enters the riser with rate that is determined by the slide valve at the end of the regenerator standpipe (eq.(28)) after time lag given by eq.(29):

$$\dot{W}_{C:\mathrm{RS}} = k_{\mathrm{SV_1}} \left(\frac{A_{\mathrm{SP}}{}^2 A_{t:\mathrm{SV_1}}{}^2}{A_{\mathrm{SP}}{}^2 - A_{t:\mathrm{SV_1}}{}^2} \right)^{0.5} \left(2\rho_p \left(1-\varepsilon_b\right) \left(P_{\mathrm{RG}}^{(l_F=1)} + \Delta P_{\mathrm{RG}} + \Delta P_{\mathrm{SP}} - P_{\mathrm{RS}}^{(l_F=1)} - \Delta P_{RS} \right) \right)^{0.5} \tag{28}$$

$$t_{dead}^{(\mathrm{RG}\rightarrow\mathrm{RS})} = \frac{V_{\mathrm{SP}} \rho_p \left(1-\varepsilon_b\right)}{\dot{W}_{C:\mathrm{RG}}^{(l_D=0)}} \tag{29}$$

The same formulation is used to calculate the catalyst mass flow rate entering the regenerator after time lag determined by the residence time of the catalyst in the liftline:

$$\dot{W}_{C:\mathrm{RG}}^{(l_D=1)} = k_{\mathrm{SV}_2}\left(\frac{A_{\mathrm{ST}}{}^2 A_{t:\mathrm{SV}_2}{}^2}{A_{\mathrm{ST}}{}^2 - A_{t:\mathrm{SV}_2}{}^2}\right)^{0.5}\left(2\rho_p\left(1-\varepsilon_{mf}\right)\left(P_{\mathrm{ST}}^{(l_F=1)} + \Delta P_{\mathrm{ST}} - P_{\mathrm{RG}}^{(l_F=1)} - \Delta P_{\mathrm{LL}}\right)\right)^{0.5} \tag{30}$$

$$t_{dead}^{(\mathrm{SP}\rightarrow\mathrm{RG})} = \frac{V_{\mathrm{LL}}\rho_p\left(1-\varepsilon_{mf}\right)}{\dot{W}_{C:\mathrm{ST}}^{(l_D=0)}} \tag{31}$$

The industrial practice for profitable and constant operation of the FCC unit is to control the riser exit temperature. The automatic control of the reactor temperature was included in the simulator with a routine that adjusts the catalyst circulation rate for constant riser temperature. Using the pseudo-steady state model of the riser, the catalyst circulation rate is regulated by solving the system provided by the heat balance (eq.(3)) and the conversion and coke yield equations (eqs.(1),(2)) simultaneously, at each solution cycle, as shown in Fig. 4. In Fig. 4 the regenerator temperature, the riser temperature, the coke on regenerated catalyst, the rate and quality of the feedstock, and the inerts rate are used for the calculation of the catalyst circulation rate that redeems the mass and energy balances in the riser. Based on the new calculated value for the catalyst circulation rate and the estimate of coke production, the stripper entrance variables and the regenerator exit flow are updated and the loop continues, until the convergence that declares the imposition of steady state is achieved.

Model Application to the pilot plant of CPERI

The responses of the simulator were recorded for step changes in the flow rate and preheat temperature of the feed. For the needs of this particular study experiments were performed with the controller of reactor temperature by catalyst circulation rate set to operation or not, in order to examine the open and closed loop behavior of the unit. Accordingly, the part of the simulator that adjusts the catalyst circulation rate for constant riser temperature was set active or inactive. The open loop experiments were used for validation of the mass and energy balances formulation and for verification of the structure of the integrated model (assumption of pseudo-steady state operation of the riser, iterative procedure of convergence etc.). In the open loop experiments the actions of the controller of riser temperature-catalyst circulation rate do not interfere with the process dynamics and the net dynamic responses of the unit to the changes in the manipulated variables can be observed. The closed loop experiments were performed to examine the effect of the controller of riser temperature-catalyst circulation rate on the behavior of the unit and were compared with the dynamic model responses, with the routine of adjustment of catalyst circulation rate being active. All experiments were performed with constant feedstock and catalyst, the properties of which are presented in Table 3.

In the next paragraphs the four cases examined are presented. First, the open loop responses of the unit and the simulator to a 15% decrease in feed flow rate are presented. Second, the responses of the simulator are compared with those of the unit for the same change, but in closed loop operation. The last two cases examine the effect of increasing the feed preheat temperature to 130% of its original value in open and closed loop operation. At this point it should be noted that the pilot plant shows a great deviation from the ideal instantaneous step change that the operator orders. The 15% decrease in feed rate was established in the real time operation of the pilot plant within a 5 min period; while an average of 80 min was required for the 130% increase of the feed preheat temperature. The main duty of the pilot plant of

CPERI is to perform steady state experiments in standard conditions for the evaluation of new catalysts, thus the observed high delays in imposing changes in the manipulated variables is understandable and justified. At this point the development of the dynamic simulator focuses on the study of the integrated riser-regenerator system; hence it does not include models for the feed mass flow meter and the heater. The transients in the imposition of the changes in question were, however, recorded by the control system of the pilot plant. Thus, it was possible to reproduce the transients of change in the manipulated variables in five consecutive representative steps, as shown in Figures 5(a)-8(a). These representative step changes are the very fact of what was called "step change" in this study and these were entered to the simulator.

Feed rate 15% decrease - open loop operation

Experimental details: In the first experiment the standpipe slide valve was set to manual mode, equal to its average opening of the previous one hour steady state operation. The time this action was taken is marked with the first vertical dotted line in diagrams of Fig. 5. Average values in non-linear systems produce momentary instabilities; hence a line-out period of 10 min was needed. When the unit reached steadiness (second vertical dotted line in diagrams of Fig. 5), a step change in the feed mass flow was imposed (from 15.5 to 12.8 gr/min), which produced the transient in feed flow rate shown in Fig. 5(a). The feed flow rate that was entered to the simulator represented this transient by the consecutive step changes shown in Fig. 5(a). After a period of 20 min, the pattern of changes of Fig. 5(a) was manually imposed to the stripper slide valve. The specific oscillatory pattern was chosen to distinct the effect of catalyst circulation rate, without considerably alter the pressure balance of the unit.

Effect of change in feed rate: The decrease in feed rate caused an instantaneous increase in the riser temperature (Fig. 5(b)), because less feed consumed less heat for vaporization. Furthermore, the catalyst to oil ratio increased, since the catalyst circulation rate was the same

(open loop operation) and the feed rate lower. The latter resulted in higher conversion and coke yield (feed basis) observed and predicted, as shown in Table 4. However, the coke rate entering the regenerator decreased, because the feed rate was lower. This produced a decrease in the regenerator temperature (Fig. 5(b)). As shown Fig. 5(c) the lower coke rate entering the regenerator resulted in a decrease in the CO_2 and SO_2 concentration and a parallel increase of the excess O_2.

Effect of change in catalyst flow: The comparison of Fig. 5(a), (b) and (c) shows that the oscillation in the catalyst flow rate, produced by the changes in the stripper slide valve opening, showed a more pronounced effect on flue gas composition than on regenerator temperature. Evidently, the many factors involved in the regenerator heat balance (temperature and flow of catalyst and gas entering and exiting the regenerator, dense bed volume, heat loss) result in smoother transients of the regenerator temperature. The decrease in regenerator temperature led to a smaller decrease in standpipe temperature (Fig. 5(e)), which again resulted to an even smaller decrease in riser temperature (Fig. 5(b)). The loop was continued for a period of 100 min (third vertical dotted line in diagrams of Fig. 5), until convergence. The variation of the stripper slide valve opening led to implicit variation of the stripper pressure drop (Fig. 5(d), without a parallel variation of the regenerator bed height. The reason for this is the much larger regenerator diameter. The change in regenerator temperature and the small variation of the catalyst flow rate resulted in the temperature profiles of liftline and standpipe shown in Fig. 5(e). The simulator predictions are in good agreement with the real dynamic behavior of the unit. The form of entering the step change in five representational consecutive steps has a negligible effect in the simulation of the unit dynamic responses. In open loop operation the simulator can predict the dynamic behavior of the pilot plant in terms of temperature, yield of combustion reactions, and pressure, which are the variables that can be measured on-line.

Feed rate 15 % decrease - closed loop operation

Experimental details: In this case the previous experiment was repeated (Fig. 6(a)), but for closed loop operation of the unit. The standpipe slide valve was set to control the riser temperature and the stripper slide valve operated for constant stripper pressure drop. Accordingly, the routine of the simulator that adjusts the catalyst circulation for constant riser temperature was activated, while the catalyst rates at the entrance and the exit of the stripper were set equal. The simulation results are of course quite different from the actions of the controllers, which are much slower. Thus, the results of the simulator are examined in the sense of an "ideal efficiency controller". Nonetheless, the steady states and the general trends of the simulator and the pilot plant should be similar.

Effect of change in feed rate: The decrease in feed rate should have produced an increase in riser temperature, though the controller (or the adjustment routine) lowered the catalyst circulation rate to satisfy the heat balance of the riser for temperature equal to 526.8°C. The first regenerator response predicted by the simulator is a minor temperature increase, owed to the lower cold catalyst mass entering- and hot catalyst mass exiting the regenerator. Thereafter, the regenerator temperature decreased due to the lower coke rate that decreased the exothermic combustion reactions. As shown in Fig. 6(b), the phenomenon was quite different in the unit. The standpipe slide valve controller is not efficient enough to balance the catalyst circulation rapidly, thus it produced an oscillation in the riser temperature for a period of 90 min. Moreover, the stripper bed height oscillated around its average value (Fig. 6(c)), whereas the regenerator bed height was again relatively constant, owing to its larger diameter. As shown in Fig. 6(c) and (d) the results of the simulator are straightforwardly comparable with the results of the pilot plant, yet the simulator is "faster". The final steady state was achieved after 100 min in the unit, while a transient of only 40 min is predicted by the simulator. This is a typical example of how such a simulator can help towards the direction of

optimal unit control, if for instance the demand was for constant riser temperature and minimum transition time.

Feed preheat temperature 130% increase - open loop operation

Experimental details: In this case the effect of increasing the feed preheat temperature from 104°C to 232°C on the dynamic performance of the pilot plant in open loop operation was explored. At the time marked with the first vertical dotted line in diagrams of Fig. 7, the standpipe slide valve was set to manual mode. After a line-out period of 30 min (second vertical dotted line in diagrams of Fig. 7), the step change was imposed to feed preheat zones 1 and 2, which produced the transient in feed preheat temperature shown in Fig. 7(a). The long transient of preheat change was represented, for the simulator needs, by the consecutive step changes shown in Fig. 7(a). In this case the stripper slide valve opening was set constant.

Effect of change in feed preheat: The increase in feed preheat temperature caused an instant increase in the riser temperature as the heat balance of the riser imposes (Fig. 7(b)). This increase in riser temperature led to higher feed conversion but not different coke yield (Table 5), since coke production is not significantly influenced by temperature. The method of representing the transient of change in feed preheat with consecutive steps is less accurate in this case. However, the general trends of the pilot plant and the simulator are similar (Fig. 7(b)). As shown in Fig. 7(b) and (e), there is a deviation of 2-5°C in the prediction of regenerator and standpipe temperature. This is not followed by a difference in the flue gas composition, which was predicted and observed relatively constant (Fig. 7(c)). Effects of wall heaters that operate for the establishment of pseudo-adiabatic conditions could have generated this increase in regenerator and standpipe temperature and could not be depicted by the simulator. The pressure drop of the stripper and the regenerator were measured and predicted constant (Fig. 7(d)), as the catalyst circulation rate and coke yield did not significantly

change. As presented in Table 5, the accuracy in the prediction of the final steady state in this case is fair.

Feed preheat temperature 130% increase - closed loop operation

Experimental details: The previous experiment was repeated, but in closed loop operation of the pilot plant (Fig. 8(a)). The slide valves controllers were set to automatic operation and the routine of the simulator that adjusts the catalyst circulation for constant riser temperature was activated. The imposed change produced the transient of Fig. 8(a), which again was represented by five consecutive step changes.

Effect of change in feed preheat: The inefficiency of the standpipe slide valve controller produced an oscillation in riser temperature (Fig. 8(b)), whereas the sluggish behavior of the stripper slide valve produced large oscillation in the stripper bed height and even a small oscillation in the regenerator bed height (Fig. 8(d). The fluctuation of the catalyst stream entering the regenerator resulted in hard oscillation in the flue gas composition (Fig. 8(c)). The final steady state was achieved at a lower catalyst circulation rate and coke yield, with higher regenerator temperature as shown in Table 5. The experimental results presented in Table 5 are of moderate accuracy, as in this case the final steady state was not well established. The performance of the simulator is again "faster", yet in this case the difference between experiment and model is much more crucial. More robust control could definitely enhance the steadiness in the operation of the unit and would produce smother profiles in critical unit variables as the riser temperature and the regenerator flue gas. The response of the simulator proposes that it could be possible with optimal control to set the regenerator to absorb the increase in the feed preheat temperature and preserve the riser temperature constant at 526°C with smooth unit performance.

Conclusions

A dynamic simulator of the FCC integrated riser-regenerator system was presented. The nonlinear dynamic and multivariable model was verified with a set of dynamic experiments performed in the pilot plant of CPERI. The term "dynamic experiments" is used to express experiments, in which a step change is imposed to a manipulated process variable, while recording the transient of a number of process variables from the current steady state to the new steady state the system will eventually reach, in both open and closed loop operation. The simulator performs satisfactorily, in describing the complex responses of the unit to typical disturbances. Increases in the riser input variables corresponded to aggressive responses of the system, since the riser has a very small contribution to the dynamic behavior of the integrated system. However, after the immediate new state was reached, the regenerator led the system to the new steady state in much greater times. The excellent convergence between observed and predicted values for reactor and regenerator temperatures indicates the accurate formulation of the mass and energy balances. The results of both the simulator and the pilot plant are in excellent agreement with the experience of real-time operation of FCC units. The accurate simulation of the pilot plant is significant for process optimization studies. The ultimate scope of this study is to utilize the simulator as a basis for model based control of the pilot plant. The purpose of such a controller would be to provide the operator with the ability of driving the pilot process to desired states, such as the maximization of the selectivity of a desired product or the maximization of the process conversion.

Acknowledgement

Financial support by the Ministry of National Education and Religious Affairs (program 2.2.01 ARCHIMIDES I, EPEAEK II) and the General Secretariat of Research and Technology Hellas (program AKMON 01) is gratefully acknowledged.

Nomenclature

A	cross-sectional area (m^2)
c, c_x	total coke yield wt%, catalytic coke yield wt%
C_A	aromatic carbon content wt% of feed
CCR	conradson carbon residue wt% of feed
D	diameter (m)
d_p	catalyst particle mean diameter (m^3)
cp	specific heat (kcal/molK)
E_x, E_c	activation energy of reaction to x, c (kcal mol^{-1})
f_b, f_e	bubble, emulsion phase volume fraction
F_{ib}	molar rate in bubble (mol s^{-1})
c_{ie}	molar concentration in emulsion (mol s^{-1})
F_{if}	molar rate in freeboard (mol s^{-1})
H_t	bubble-emulsion heat interchange (kcal m^{-3} s)
K_H	heat interchange rate group (kcal m^{-3} s)
K_{Mi}	mass interchange rate group (mol m^{-3} s)
K_{Rjb}	reaction rate group of reaction j - bubble phase (mol m^{-3} s)
K_{Rje}	reaction rate group of reaction j - emulsion phase (mol m^{-3} s)
K_{Rjf}	reaction rate group of reaction j - freeboard (mol m^{-3} s)
K_{SV1}, K_{SV2}	characteristic constant of slide valve SV1, SV2
K_{ti}	bubble-emulsion gas interchange coefficient (s^{-1})
k_x, k_c	pre-exponential factor of reaction to x, c
L	height (m)
l	dimentioneless height
MW_F	feed molecular weight
N_C	carbon number in the average feed molecule

n_x, n_c	catalyst decay exponent of reaction to x, c
N_N	nitrogen number in the average feed molecule
N_T	total nitrogen content wt% of feed
Q_b	enthalpy rate in bubble phase (kcal s^{-1})
Q_C	enthalpy rate of catalyst (kcal s^{-1})
Q_{ge}	enthalpy rate of gas in emulsion phase (kcal s^{-1})
Q_{loss}	heat loss from the dense bed (kcal s^{-1})
P	pressure (Pa)
S	sulfur content wt% of feed
T_e	temperature of emulsion phase (kcal s^{-1})
T_{RX}	riser reactor temperature (°F)
t_C	catalyst residence time (s)
t_{dead}	time lug in standpipe or liftline (s)
u_g	superficial gas velocity (m s^{-1})
u_t	catalyst particle terminal velocity (m s^{-1})
V	volume (m^3)
$WHSV$	weight hourly space velocity (hr^{-1})
$\dot{W}_C$	catalyst circulation rate (kg s^{-1})
$\dot{W}_F$	gas-oil feed rate (kg s^{-1})
x	gas-oil conversion wt%
ΔH_{crack}	heat of catalytic cracking (kcal kg^{-1})
ΔH_{Rj}	heat of reaction j (kcal mol^{-1})

Greek Letters

α_{ij}	stoichiometric coefficient of component i in rection j
ε_b	voidage of bulk catalyst
ε_{mf}	voidage at minimum fluidization

ε_e dense bed emulsion void fraction

ε_f freeboard void fraction

ε_r riser void fraction

ρ_p catalyst density (kg m^{-3})

Subscripts

g gas phase

b bubble phase

e emulsion phase

f dilute phase

Unit Section Subscripts

D dense phase or bottom section

C cone intermediate section

F dilute phase or top section

CY regenerator cyclone

RS riser

RG regenerator

ST stripper

SP standpipe

LL liftline

Appendix A: Hydrodynamic Correlations and Pressure Balance

Simulation of Riser

The weight hourly space velocity (*WHSV*) and the solids residence time (t_s) were calculated by eqs.(32) and (33), following the pilot riser geometry, that is divided in three regions:

$$WHSV = \frac{\dot{W}_{F:\mathrm{RS}}}{\rho_p \left(V_{D:\mathrm{RS}} \left(1-\varepsilon_{D:\mathrm{RS}}\right) + V_{C:\mathrm{RS}} \left(1-\varepsilon_{C:\mathrm{RS}}\right) + V_{F:\mathrm{RS}} \left(1-\varepsilon_{F:\mathrm{RS}}\right) \right)} \tag{32}$$

$$t_{C:\mathrm{RS}} = \frac{3600}{WHSV} \frac{\dot{W}_{F:\mathrm{RS}}}{\dot{W}_{C:\mathrm{RS}}} \tag{33}$$

(a) The mixing region at the riser bottom. The void fraction ($\varepsilon_{D:\mathrm{RS}}$) and subsequently the catalyst inventory of this region, were related to the superficial gas velocity by means of the empirical correlation of Richardson and Zaki (Richardson & Zaki, 1954) (eq.(34)), which substantiates for a dense regime in the bottom region of the pilot unit.

$$\varepsilon_{D:\mathrm{RS}} = \left(\frac{u_{g:D:\mathrm{RS}}}{u_{t:\mathrm{RS}}} \right)^{1/z} \tag{34}$$

(b) The conical shaped intermediate region. Because of the very small volume of the intermediate region (15% of total riser volume), a simple approximation of averaged (between top and bottom regions) hydrodynamic attributes was used (Pugsley & Berruti, 1996).

(c) The fast fluidization region at the riser top, which was simulated under the following assumptions: (i) the flow is fully developed, thus its hydrodynamic features remain constant with height; (ii) the total volumetric yield of the reaction is flowing through the whole height of this region; (iii) the particle acceleration is considered to be negligible. Hence, eq.(35) holds:

$$\varepsilon_{F:\mathrm{RS}} = \frac{u_{g:F:\mathrm{RS}} \rho_p A_{F:\mathrm{RS}}}{y_{F:\mathrm{RS}} \dot{W}_{C:\mathrm{RS}} + u_{g:D:\mathrm{RS}} \rho_p A_{F:\mathrm{RS}}} \tag{35}$$

In eq.(35) $y_{F:\mathrm{RS}}$ is the average gas-solids slip factor for the top section of the riser, which was proven to play an important role in small diameter riser reactors (Bollas et al., 2002). The

correlation of Pugsley et al. (Pugsley & Berruti, 1996) was applied for the estimation of the gas-solids slip factor as shown in eq.(36), where Fr_g and Fr_t are the *Froude* numbers for the superficial gas velocity and solids terminal velocity, respectively:

$$y_{F:\mathrm{RS}} = 1 + \frac{5.6}{Fr_{g:F:\mathrm{RS}}^2} + 0.47 Fr_{t:F:\mathrm{RS}}^{0.41} \tag{36}$$

A detailed pressure gradient analysis is required for small diameter risers (Bollas et al., 2002). For this analysis, all pressure gradients should be taken into account, and eq.(37) is valid where ΔP_{fg} is the gas-wall frictional pressure drop, ΔP_{fs} is the solids-wall frictional pressure drop, ΔP_{acc} is the pressure drop due to solids acceleration, and the other terms represent the pressure drop due to solids and gas static head throughout the total riser height:

$$\Delta P_{\mathrm{RS}} = \Delta P_{fg:\mathrm{RS}} + \Delta P_{fs:\mathrm{RS}} + \Delta P_{acc:\mathrm{RS}} + \varepsilon_{\mathrm{RS}} \rho_{g:\mathrm{RS}} g L_{\mathrm{RS}} + \left(1 - \varepsilon_{\mathrm{RS}}\right) \rho_p g L_{\mathrm{RS}} \tag{37}$$

Simulation of Regenerator

For group A particles the emulsion gas superficial velocity is the gas velocity for zero net flow of solids, which equals the minimum bubbling velocity, plus (concurrent gas/solids flows) or minus (countercurrent gas/solids flow) the superficial solids velocity in the emulsion phase:

$$u_{ge} = u_{mb} \pm u_{se} \tag{38}$$

For the evaluation of the minimum fluidization velocity the equation of Wen and Yu (Kunii & Levenspiel, 1977) is applied. For group A particles the minimum bubbling velocity, u_{mb}, is evaluated by the correlation of Abrahamsen and Geldart (Abrahamsen & Geldart, 1980), which considers the effect of catalyst fines, f, on u_{mb}:

$$\frac{u_{mb}}{u_{mf}} = \frac{2300 \rho_{ge}^{\ 0.126} \mu_{ge}^{\ 0.523} \exp\left(0.716 f\right)}{d_p^{\ 0.8} g^{0.934} \left(\rho_p - \rho_{ge}\right)^{0.934}} \tag{39}$$

The superficial gas velocity in the dense zone is then obtained by eq.(40):

$$u_{g:\mathrm{RG}} = u_{gb} + u_{ge} \tag{40}$$

The fraction of the bubbles in the dense zone is:

$$f_b = \frac{u_{gb}}{\upsilon_b} \tag{41}$$

The absolute bubble rise velocity υ_b is calculated as a function the isolated bubble rise velocity:

$$\upsilon_b = 0.711\left(g d_b\right)^{0.5} + u_{g:\mathrm{RG}} - u_{ge} \tag{42}$$

The bubble diameter is estimated by the Wen-Mori correlation (Kunii & Levenspiel, 1977):

$$\frac{d_b^{(l_D=1)} - d_b}{d_b^{(l_D=1)} - d_b^{(l_D=0)}} = \exp\left(-\frac{0.3 L_{D:\mathrm{RG}} l_D}{D_{D:\mathrm{RG}}}\right) \tag{43}$$

The initial bubble diameter and the maximum bubble diameter are estimated by eqs.(26) and (27), respectively:

$$d_b^{(l_D=0)} = \frac{1.38}{g^{0.2}}\left(\frac{1}{1000}\left(u_{g:\mathrm{RG}}^{(l_D=0)} - u_{mb}\right)\right)^{0.4} \tag{44}$$

$$d_b^{(l_D=1)} = \min\left[0.652\left(A_{D:\mathrm{RG}}\left(u_{g:\mathrm{RG}}^{(l_D=1)} - u_{mb}\right)\right)^{0.4},\ 2\frac{\left(u_t^{(2.7 d_p)}\right)^2}{g}\right] \tag{45}$$

The emulsion to freeboard elutriation rate K_i^* of a fraction of particles with average diameter d_{pi} is evaluated by the Zenz and Weil correlation (Geldart, 1985). The total entrainment rate K_t^* is then obtained by adding the rates of each respective fraction of particles. The catalyst density in the freeboard is a function of the gas-solids slip velocity, which is calculated on the basis of the correlation of Patience et al. (Patience et al., 1992), as shown in eq.(46):

$$u_{sf} = \frac{u_{gf}}{1 + 5.6/Fr_{gf} + 0.47 Fr_t^{0.41}} \tag{46}$$

The freeboard voidage is then calculated by eq.(47):

$$\varepsilon_f = 1 - \frac{K_t^*}{\rho_p u_{sf}} \tag{47}$$

The pressure drop throughout the regenerator is calculated from the solids static head as shown in eq.(48):

$$\Delta P_{\mathrm{RG}} = \rho_p \left(1-\varepsilon_e\right) f_e g L_{D:\mathrm{RG}} + \rho_p \left(1-\varepsilon_f\right) g L_{F:\mathrm{RG}} \tag{48}$$

Simulation of Stripper, Standpipe, Liftline and Slide Valves

The pressure drop throughout the stripper is calculated from the solids static head as shown in eq.(49):

$$\Delta P_{\mathrm{ST}} = \rho_p \left(1-\varepsilon_{mf}\right) g L_{D:\mathrm{ST}} \tag{49}$$

The catalyst circulation throughout the unit is regulated by two slide valves, one at the riser entrance and one at the stripper exit. The catalyst circulation rate at the entrance and exit of the regenerator was correlated with the slide valves opening and pressure drop by eq.(50) (Judd & Dixon, 1978):

$$\dot{W}_C = k_{\mathrm{SV}} \left(\frac{A_0^{\,2} A_{t:\mathrm{SV}}^{\,2}}{A_0^{\,2} - A_{t:\mathrm{SV}}^{\,2}} \right)^{0.5} \left(2\rho_p \left(1-\varepsilon\right) \Delta P_{SV}\right)^{0.5} \tag{50}$$

Appendix B: The bulk molecular feedstock characterization approach

The effect of feedstock quality in eqs.(1) and (2), was simulated with a "bulk molecular characterization approach" (Bollas et al., 2004), that is the calculation of the relative (compared to a reference feedstock) potential of an FCC feedstock to enhance catalytic cracking conversion (*crackability*) and coke formation (*coking tendency*). The proposed models focus on the needs of industry; hence they include the bulk feedstock properties of Fig. 9, measured with standard analytical procedures accessible to the average refinery (Bollas et al., 2004). Fig. 9 presents the computational methodology for the breakdown of an FCC feedstock into pseudo-components and for the estimation of the

properties of light and heavy fractions, separately. This splitting and lumping scheme was applied to explore the different extent of contributions to the catalytic cracking of the heavy and the light fractions.

The bulk feedstock properties were combined properly to deliver five functional groups to characterize the behavior of FCC feedstocks at cracking conditions, which involved: the prediction of catalyst poisoning, the estimation of the cracking extent, the estimation of coke/conversion selectivity, and two coking precursors for contaminant and residue coke formation (Bollas et al., 2004), as shown in eqs.(51) and (52):

$$\frac{x}{100-x}=\left[w_1\left(N_C-N_CC_A\right)+w_2\left(N_N\right)+w_3\right]\frac{t_{C:RS}{}^{n_x}}{WHSV}\exp\left(\frac{-E_x}{RT_{RX}}\right) \tag{51}$$

$$\begin{aligned} c &= k_{CCR}CCR+k_NN_N\exp\left(\frac{-NT}{NT+0.437S}\right) \\ &+\left[\left(w_4+w_5C_A\right)^2\right]\left[w_1\left(N_C-N_CC_A\right)+w_2\left(N_N\right)+w_3\right]\frac{t_{C:RS}{}^{n_c}}{WHSV}\exp\left(\frac{-E_c}{RT_{RX}}\right) \end{aligned} \tag{52}$$

A large database of experiments performed in the FCC pilot plant of CPERI, with a standard catalyst and a large variety of feedstock qualities, was used for the development and validation of eqs.(51) and (52). Moreover, a database of experiments with different catalysts and feedstocks was used for the assignment of a “catalyst index” to each catalyst to describe the effect of catalyst quality in eqs.(1) and (2). The description of catalyst activity and selectivity with a simple index is a common strategy in industry, in order to validate catalyst performance in commercial units. The values of the parameters of eqs.(51) and (52) are given in Table 1.

Literature Cited

Abrahamsen, A.R., Geldart, D., (1980). Behaviour of gas-fluidized beds of fine powders, part I. Homogeneous expansion. *Powder Technology*, 26(1 , May-Jun. 1980), 35-46.

Ali, H., Rohani, S., (1997). Dynamic modeling and simulation of a riser-type Fluid Catalytic Cracking Unit. *Chemical Engineering & Technology*, 20(2), 118-130.

Ali, H., Rohani, S., Corriou, J.P., (1997). Modelling and control of a riser-type Fluid Catalytic Cracking (FCC) Unit. *Chemical Engineering Research & Design*, 75(A4), 401-412.

Arbel, A. et al., (1995). Dynamic and control of Fluidized Catalytic Crackers. 1. Modeling of the current generation of FCCs. *Industrial & Engineering Chemistry Research*, 34(4), 1228-1243.

Arbel, A., Rinard, I.H., Shinnar, R., (1995). Dynamics and control of Fluidized Catalytic Crackers. 2. Multiple steady-states and instabilities. *Industrial & Engineering Chemistry Research*, 34(9), 3014-3026.

Arthur, J.R., (1951). Reactions between carbon and oxygen. *Transactions of the Faraday Society*, 47, 164-178.

Blanding, F.H., (1953). Reaction rates in the catalytic cracking of petroleum. *Industrial & Engineering Chemistry*, 45, 1186.

Bollas, G.M. et al., (2002). Modeling small-diameter FCC riser reactors. A hydrodynamic and kinetic approach. *Industrial & Engineering Chemistry Research*, 41(22), 5410-5419.

Bollas, G.M. et al., (2004). Bulk Molecular Characterization Approach for the simulation of FCC feedstocks. *Industrial & Engineering Chemistry Research*, 43(13), 3270-3281.

Cristea, M.V., Agachi, S.P., Marinoiu, V., (2003). Simulation and model predictive control of a UOP fluid catalytic cracking unit. *Chemical Engineering And Processing*, 42(2), 67-91.

Davidson, J.F., Clift, R., Harrison, D. (1985). *Fluidization.* Academic Press Inc., London.

Elnashaie, S., Elshishini, S.S., (1993). Digital-Simulation of industrial Fluid Catalytic Cracking Units. 4. Dynamic behavior. *Chemical Engineering Science*, 48(3), 567-583.

Elnashaie, S., Abasaeed, A.E., Elshishini, S.S., (1995). Digital-Simulation of industrial Fluid Catalytic Cracking Units. 5. Static and dynamic bifurcation. *Chemical Engineering Science*, 50(10), 1635-1644.

Faltsi-Saravelou, O., Vasalos, I.A., (1991). Fbsim - A model for fluidized-bed simulation. 1. Dynamic modeling of an adiabatic reacting system of small gas-fluidized particles. *Computers & Chemical Engineering*, 15(9), 639-646.

Faltsi-Saravelou, O., Vasalos, I.A., Dimogiorgas, G., (1991). Fbsim - A model for fluidized-bed simulation. 2. Simulation of an industrial fluidized catalytic cracking regenerator. *Computers & Chemical Engineering*, 15(9), 647-656.

Geldart, D., (1973). Types of gas fluidization. *Powder Technology*, 7(5), 285-292.

Geldart, D. (1985). Elutriation, in Davidson, J.F., Clift, R. & Harrison, D. (Eds.), *Fluidization*. Academic Press Inc., London, p. 383.

Han, I.S., Chung, C.B., (2001a). Dynamic modeling and simulation of a fluidized catalytic cracking process. Part I: Process modeling. *Chemical Engineering Science*, 56(5), 1951-1971.

Han, I.S., Chung, C.B., (2001b). Dynamic modeling and simulation of a fluidized catalytic cracking process. Part II: Property estimation and simulation. *Chemical Engineering Science*, 56(5), 1973-1990.

Hernandez-Barajas, J.R., Vazquez-Roman, R., Salazar-Sotelo, D., (2006). Multiplicity of steady states in FCC units: effect of operating conditions. *Fuel*, 85(5-6), 849-859.

Howard, J.B., Williams, G.C., Fine, D.H. (1973). Kinetics of Carbon Monoxide Oxidation in Post Flame Gases. In *14th Symposium (International) on Combustion*, Pittsburgh, The Combustion Institute.

Jacob, S.M. et al., (1976). Lumping and reaction scheme for Catalytic Cracking. *Aiche Journal*, 22(4), 701-713.

Judd, M.R., Dixon, P.D., (1978). Flow of fine, dense solids down a vertical standpipe. *AIChE Symp Ser*, 74(176), 38-44.

Kesler, M.G., Lee, B.I., (1976). Improve prediction of enthalpy of fractions. *Hydrocarbon Processing*, 55(3), 153-158.

Kunii, D., Levenspiel, O. (1977). *Fluidization Engineering.* Robert E. Krieger Publishing Company Inc., Florida.

Lee, E., Groves, F.R., Jr., (1985). Mathematical model of the Fluidized Bed Catalytic Cracking Plant *Trans. Soc. Comput. Simul. Int.*, 2(3), 219-236

Lopez-Isunza, F., (1992). Dynamic modeling of an industrial Fluid Catalytic Cracking Unit. *Computers & Chemical Engineering*, 16, S139-S148.

McFarlane, R.C. et al., (1993). Dynamic simulator for a Model-IV Fluid Catalytic Cracking Unit. *Computers & Chemical Engineering*, 17(3), 275-300.

Morley, K., De Lasa, H.I., (1987). On the determination of kinetic parameters for the regeneration of cracking catalyst. *Canadian Journal of Chemical Engineering*, 65(5), 773-777.

Patience, G.S. et al., (1992). Scaling considerations for circulating fluidized bed risers. *Powder Technology*, 72(1), 31-37.

Pugsley, T.S., Berruti, F., (1996). A predictive hydrodynamic model for circulating fluidized bed risers. *Powder Technology*, 89(1), 57-69.

Richardson, J.F., Zaki, W.N., (1954). Sedimentation and Fluidization. I. *Transactions of the Institution of Chemical Engineers*, 32, 35.

Tone, S., Miura, S.I., Otake, T., (1972). Kinetics of oxidation of coke on silica-alumina catalysts. *Bull. Jap. Petrol. Inst.*, 14(1), 76.

Voorhies, A., (1945). Carbon formation on catalytic cracking. *Industrial & Engineering Chemistry*, 37, 4.

Wang, G.-x. et al., (1986). Kinetics of combustion of Carbon and Hydrogen in carbonaceous deposits on zeolite-type cracking catalysts. *Industrial & Engineering Chemistry, Process Design and Development*, 25(3), 626-630.

List of Tables

Table 1: Parameters of the model of the pilot riser

Operating Conditions		Effect of Feedstock		Heat of Cracking	
k_x	200.04	w_1	0.0261	α_1	3.49
E_x	8.9	w_2	5.6899	α_2	18.6
n_x	-0,78	w_3	0.6512	α_3	0.021
k_c	1.283	w_4	0.0317	b_1	-9.50
E_c	0.9	w_5	0.0442	b_2	53.4
n_c	-0.90	k_{CCR}	0.3000	b_3	0.044
		k_N	0.3214		

Table 2: Parameters of the model of the regenerator

Frequency Factor		Activation Energy (kcal mol^{-1})		Reference
$k_{01}+k_{02}$	1.4E05	E_1	29.9	(Morley & De Lasa, 1987)
k_{01}/k_{02}	2.5E03	E_2	12.4	(Arthur, 1951)
k_{03}	1.3E03	E_3	30.0	(Howard, Williams & Fine, 1973)
k_{04}	3.5E03	E_4	13.8	(Tone, Miura & Otake, 1972)
k_{05}	3.3E07	E_5	37.7	(Wang et al., 1986)
k_{06}	1.4E05	E_6	29.9	(Faltsi-Saravelou, Vasalos & Dimogiorgas, 1991)

Table 3: Bulk properties of the feedstock and the catalyst used in the experiments examined

Feedstock Properties		Catalyst Properties	
Code Name	#19	*Code Name*	#43
Gravity (API)	18.9	*Bulk Density ($kg\,m^{-3}$)*	900
Refractive index (at 20°C)	1.5226	*Mean Particle Diameter (μ)*	75
Sulfur %wt	2.58	*Al_2O_3, wt%*	39.1
Nitrogen %wt	0.13	*SiO_2, wt%*	59.6
Carbon %wt	85.3	*Re_2O_3, wt%*	0.65
Con. carbon residue %wt	0.36	*Fe, wt%*	0.59
TBP distillation (°C)		*Particle size distribution*	
IBP	303.6	*fraction (wt%)*	*size (μ)*
10%	379.2	*0*	
30%	422.9	*10*	
50%	454.4	*50*	
70%	483.1	*80*	
90%	524.2	*90*	
FBP	551.6	*100*	

Table 4: Steady state results (experimental and predicted) of open and closed loop behavior of the pilot plant for a 15% decrease in feed rate

	open loop behavior				closed loop behavior			
case examined	steady state 1		steady state 2		steady state 1		steady state 2	
feed rate (kg s^{-1})	25.19E-3		20.67E-3		25.64E-3		20.88E-3	
feed preheat (°C)	104.4		104.5		104.4		104.4	
	experimental vs. predicted operational variables				experimental vs. predicted operational variables			
catalyst to oil ratio	15.6	15.6	18.9	18.9	13.6	13.7	17.48	14.7
riser temperature (°C)	526.8		535.5	534.7	526.8		526.8	
reg. temperature (°C)	683.3	683.7	679.4	679.3	683.3	683.6	681.7	680.4
	experimental vs. predicted yields				experimental vs. predicted yields			
conversion wt% on feed	66.8	65.8	69.6	70.7	64.7	63.7	68.4	65.8
coke yield wt% on feed	5.78	5.77	6.63	6.66	5.31	5.32	6.49	5.65
carbon wt% on reg. cat.	0.035	0.030	0.020	0.21	0.013	0.019	0.015	0.012

Table 5: Steady state results (experimental and predicted) of open and closed loop behavior of the pilot plant for a 130% increase in feed

	open loop behavior				closed loop behavior			
case examined	steady state 1		steady state 2		steady state 1		steady state 2	
feed rate (kg s^{-1})	25.27E-3		25.25E-3		25.03E-3		25.26E-3	
feed preheat (°C)	104.4		232.4		104.4		232.3	
	experimental vs. predicted operational variables				experimental vs. predicted operational variables			
catalyst to oil ratio	14.8	14.7	15.2	14.5	13.5	13.5	12.9	11.21
riser temperature (°C)	526.8		540.6	540.9	526.7		526.7	
reg. temperature (°C)	688.1	688.8	696.8	693.9	685.4	685.3	694.4	693.3
	experimental vs. predicted yields				experimental vs. predicted yields			
conversion wt% on feed	64.7	64.7	64.9	66.4	65.2	63.53	60.5	60.28
coke yield wt% on feed	5.37	5.56	5.57	5.52	5.07	5.28	5.11	4.72
carbon wt% on reg. cat.	0.030	0.037	0.025	0.033	0.010	0.023	0.015	0.013

List of Figures

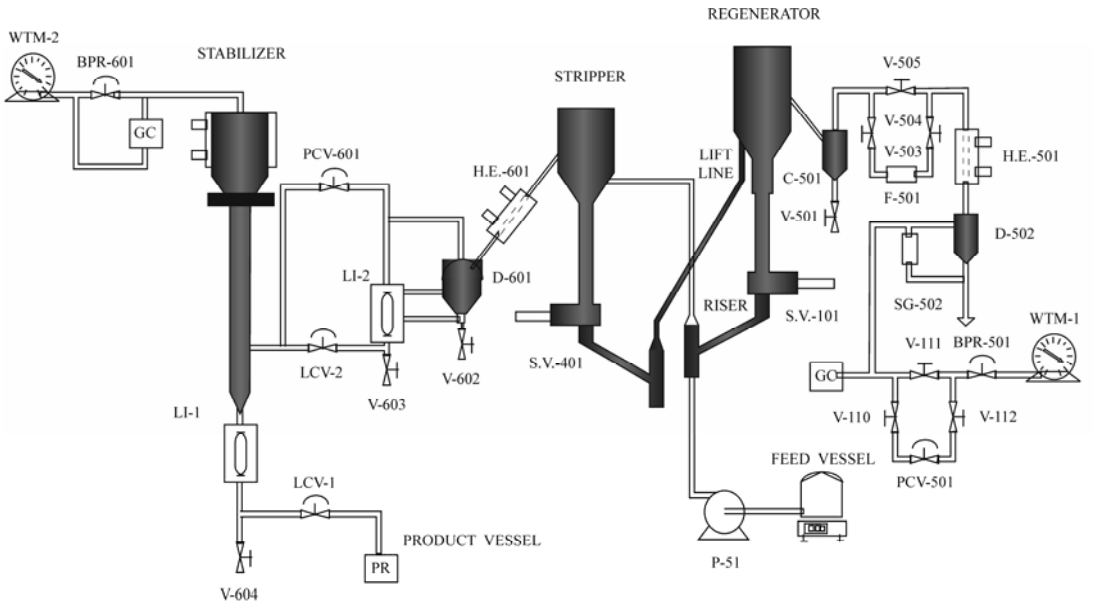

Fig. 1: Schematic diagram of the FCC pilot plant of CPERI.

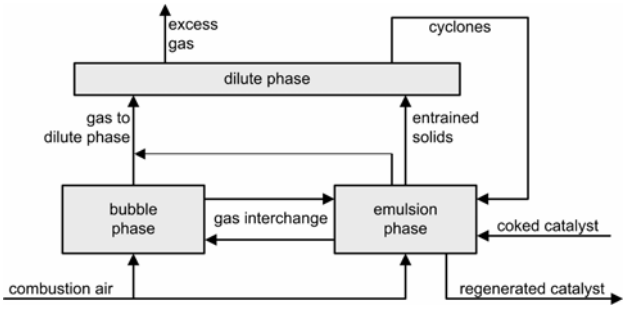

Fig. 2: Physical model of the two-phase regime used for the simulation of the regenerator.

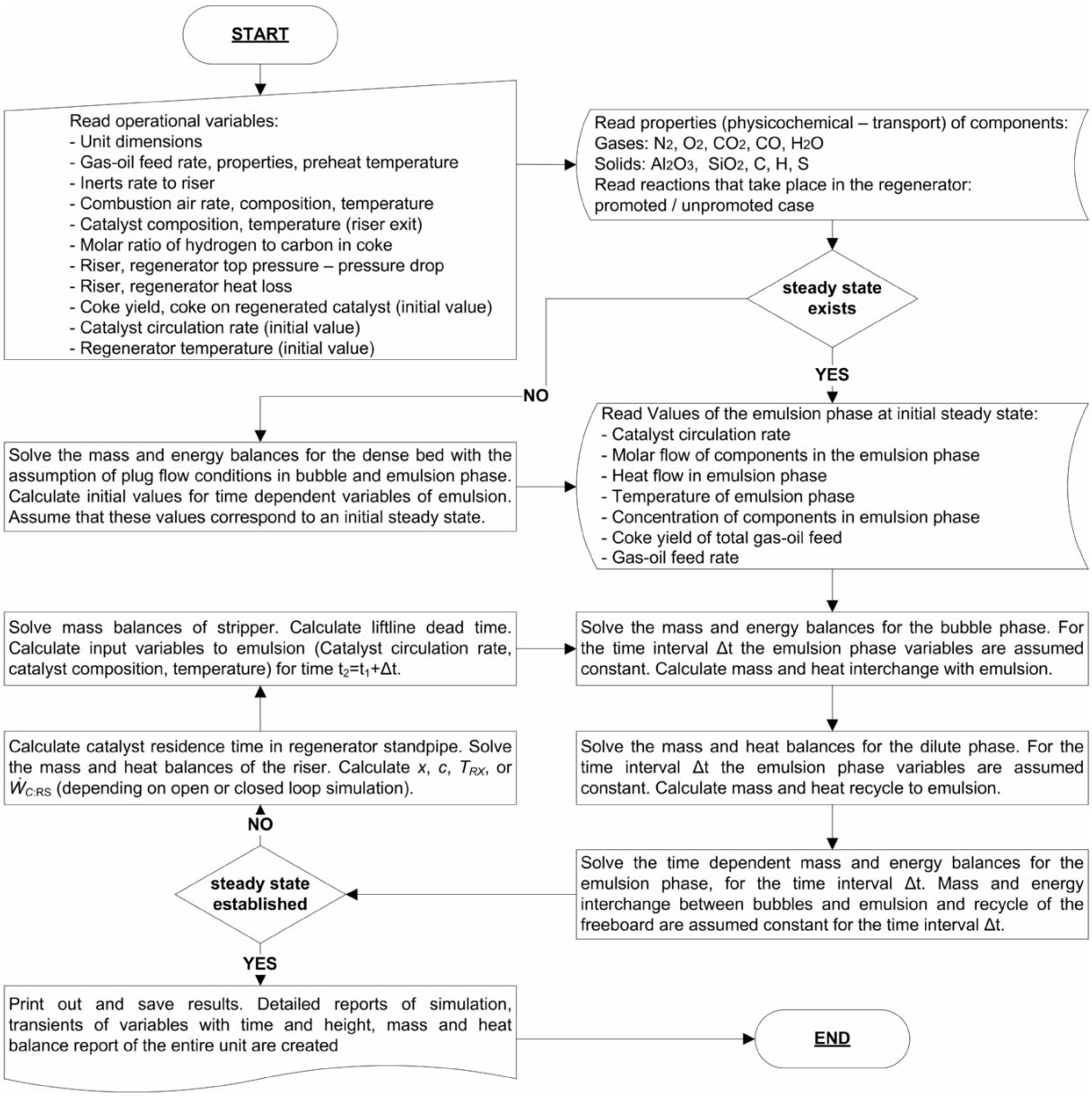

Fig. 3: Logical scheme of the dynamic simulator of the FCC pilot plant of CPERI.

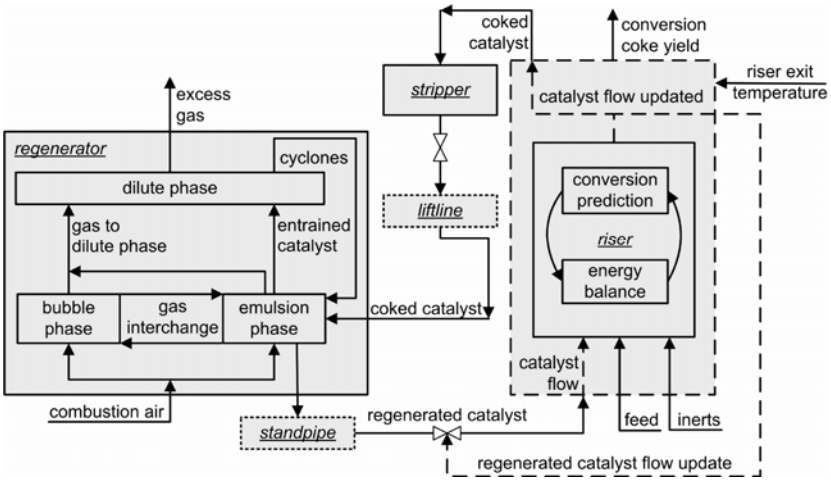

Fig. 4: Structure of solution sequence of the integrated FCC simulator.

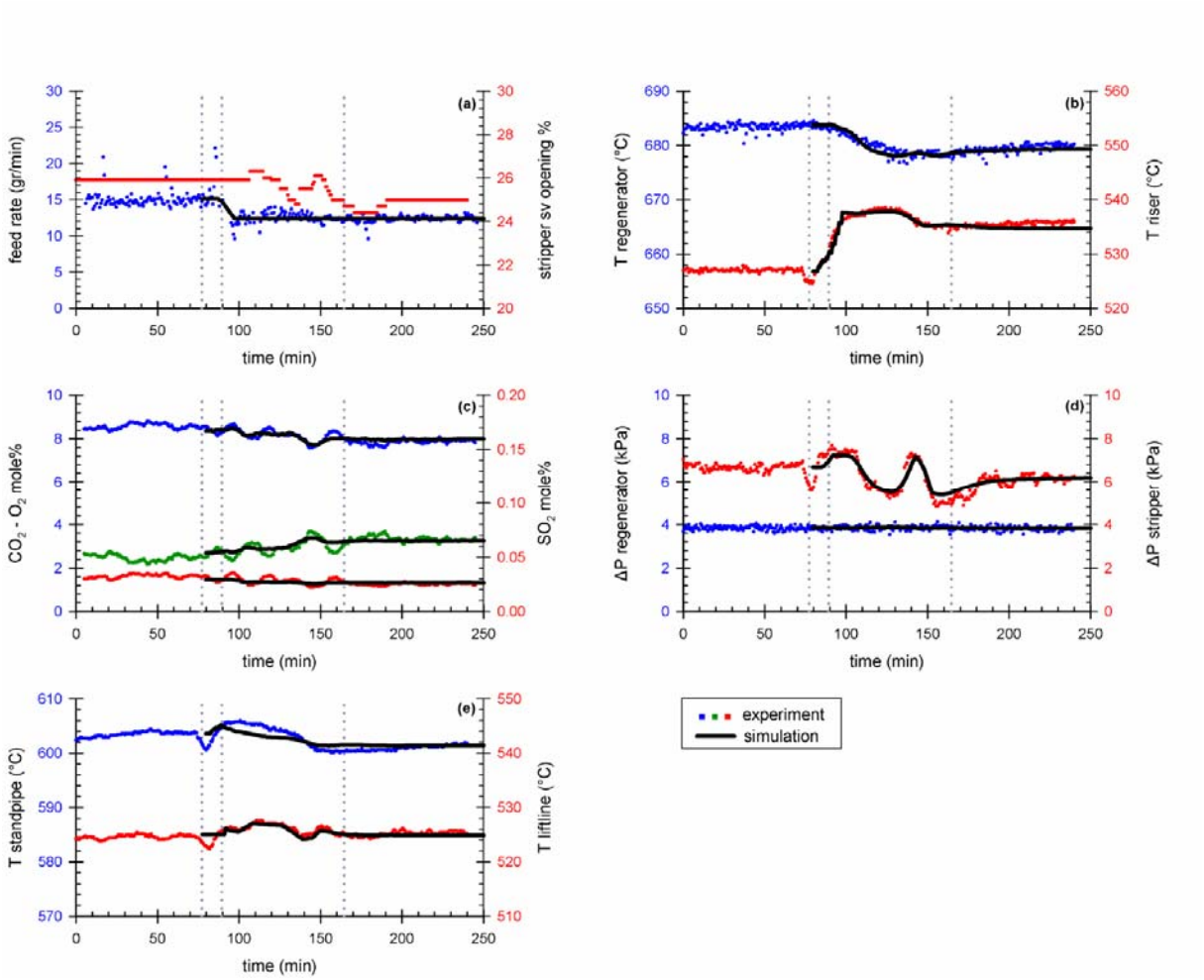

Fig. 5: Open loop responses of pilot plant and simulator for a 15% decrease in feed rate.

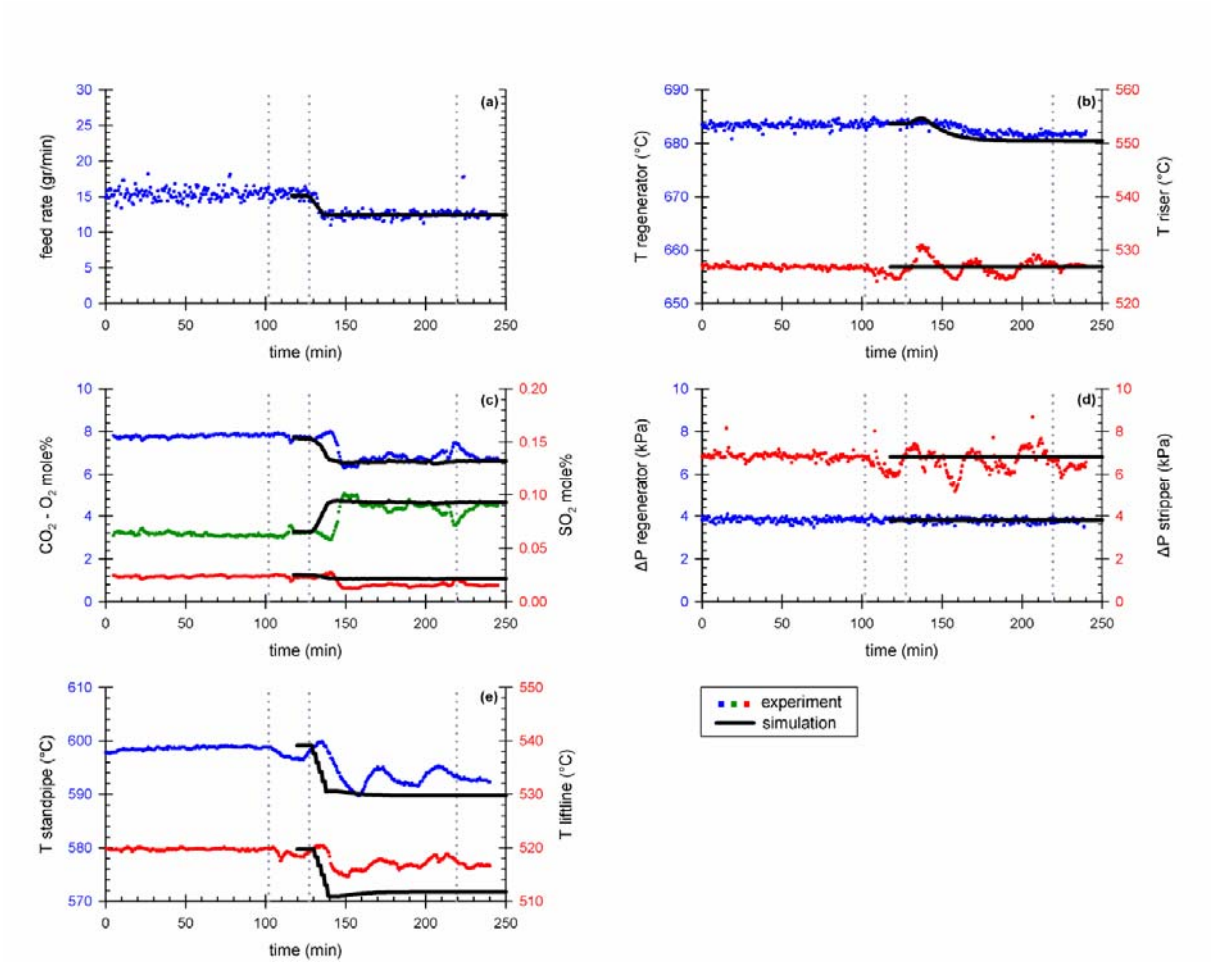

Fig. 6: Closed loop responses of pilot plant and simulator for a 15% decrease in feed rate.

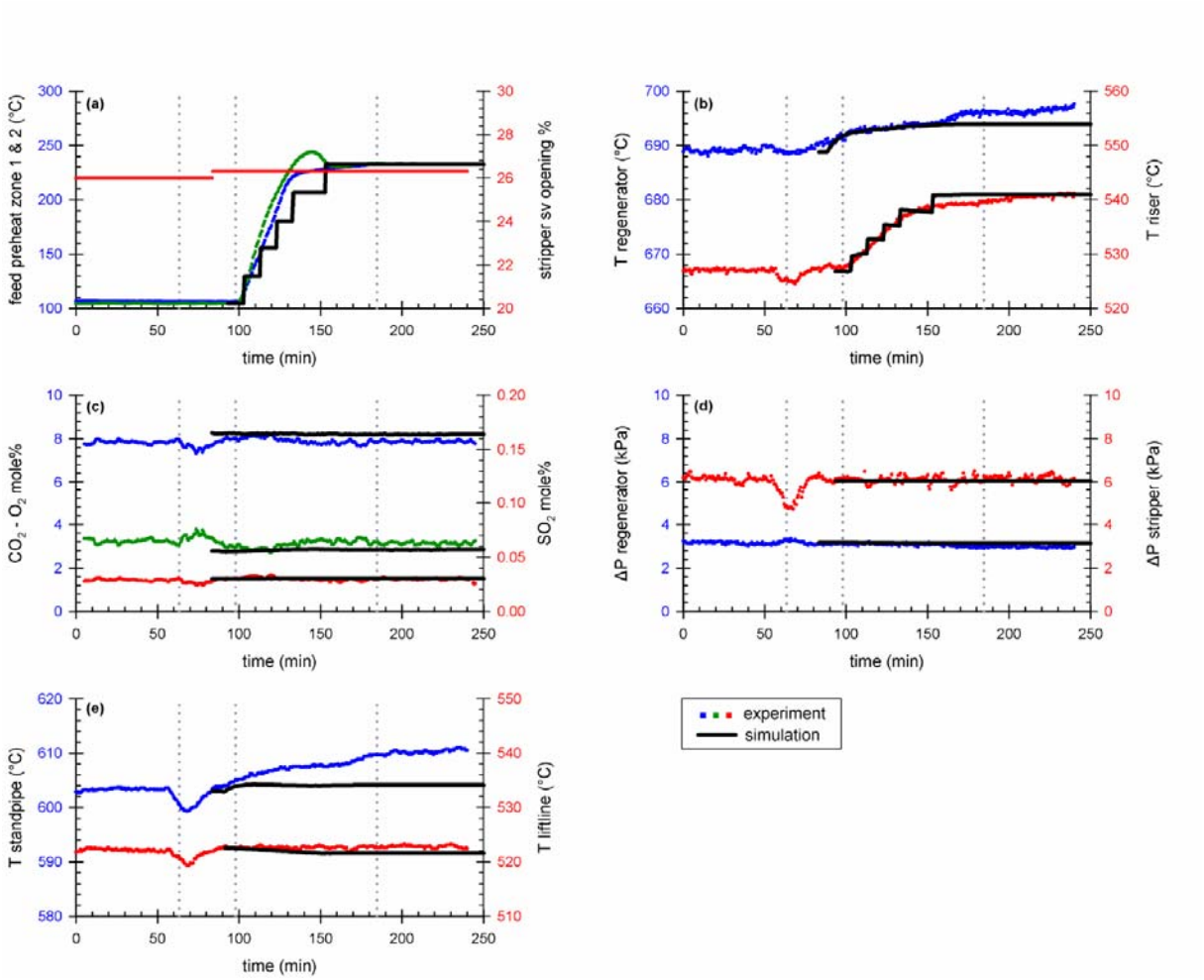

Fig. 7: Open loop responses of pilot plant and simulator for a 130% increase in feed preheat temperature.

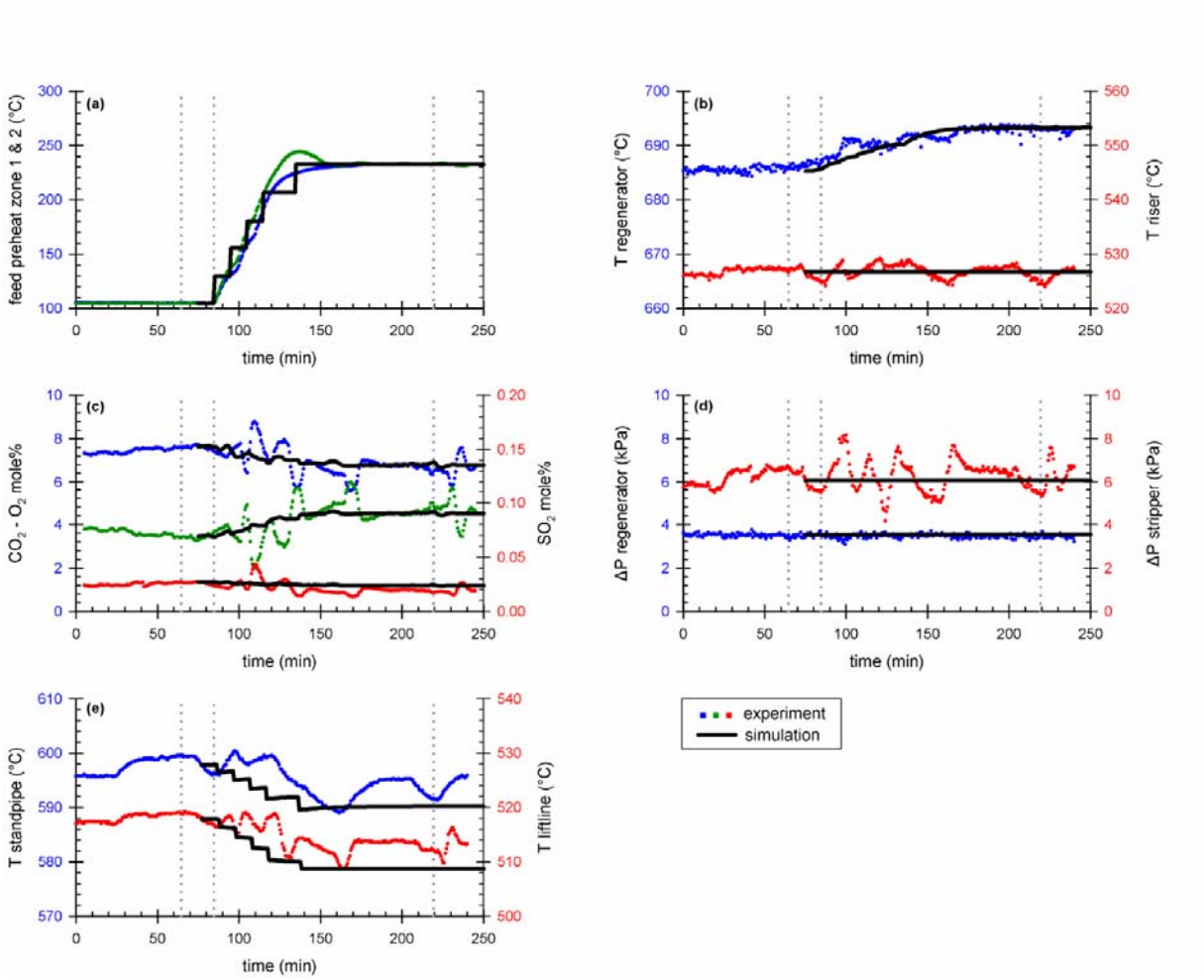

Fig. 8: Closed loop responses of pilot plant and simulator for a 130% increase in feed preheat temperature.

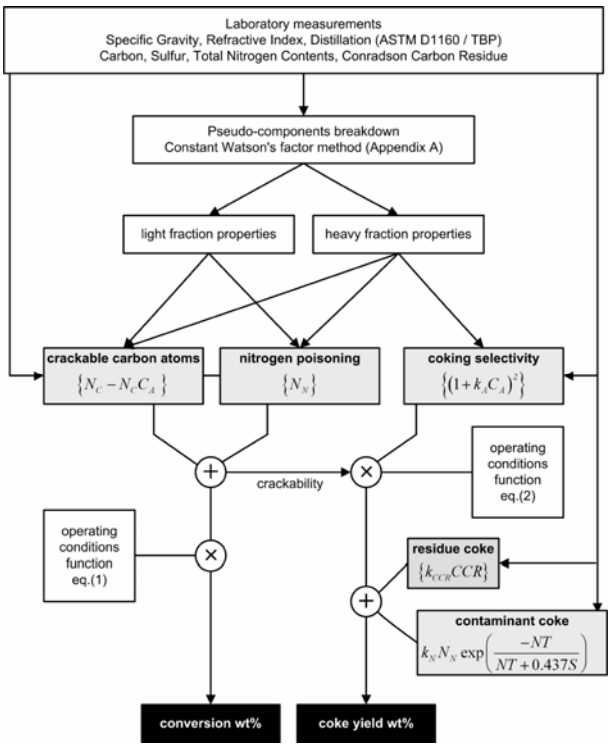

Fig. 9: Logical scheme of the proposed method for the simulation of the effect of feed properties and operating conditions on the coke yield of the FCC process.